Fibers and Polymers 2018, Vol.19, No.8, 1618-1625
DOI 10.1007/s12221-018-7953-1

ISSN 1229-9197 (print version)
ISSN 1875-0052 (electronic version)

Isolation of Nanocellulose from Water Hyacinth Fiber (WHF) Produced via Digester-Sonication and Its Characterization

Mochamad Asrofi[1], Hairul Abral[1]*, Anwar Kasim[2], Adjar Pratoto[1], Melbi Mahardika[1], Ji-Won Park[3], and Hyun-Joong Kim[3]

[1]*Department of Mechanical Engineering, Andalas University, Padang 25163, Indonesia*
[2]*Department of Agriculture Technology, Andalas University, Padang 25163, Indonesia*
[3]*Laboratory of Adhesion & Bio-Composites, Program in Environmental Materials Science, Research Institute for Agriculture & Life Sciences, Seoul National University, Seoul 08826, Korea*
(Received November 27, 2017; Revised April 5, 2018; Accepted May 2, 2018)

Abstract: The successful isolation and characterization of water hyacinth fiber (*Eichornia crassipes*) (WHF) nanocellulose is presented in this study. The novelty was in exploring a wider range of properties of highly purified samples of WHF after each stage of production in more depth. The isolation was accomplished by pulping in a digester and sonication. Morphological changes before and after treatment were demonstrated by scanning electron microscopy (SEM). The lignin and hemicellulose content decreased during chemical treatment. Transmission electron microscopy (TEM) and particle size analyzer (PSA) were used to determine the morphology of WHF after sonication for 1 h. TEM shows that the diameter and length of nanocellulose WHF were 15.61 and 147.4 nm, respectively. The crystallinity index and crystalline domain area significantly increased after chemical treatment. The highest crystallinity index was 84.87 % after an acid hydrolysis process. The increase in crystallinity leads to good thermal stability. Moisture absorption tests of WHF were carried out before and after treatment. The lowest moisture absorption was in the cellulose fiber after sonication (nanocellulose).

Keywords: Water hyacinth fiber, Nanocellulose, Pulping-digester, Sonication, Characterization

Introduction

Natural fiber obtained from plants can be used as a reinforcing agent in biopolymer composites. One such source of fiber is water hyacinth which, in the tropics, is often obtainable for free and its removal from tropical waterways has environmental advantages. Generally, natural fiber consists of three main components; cellulose, hemicellulose, and lignin [1-3]. Hemicellulose and lignin are amorphous structures which biodegrade, absorb water, and break down with heat [4]. Cellulose is a major component of natural fiber and determines its mechanical properties [3]. A higher cellulose content relates to stronger mechanical properties. Cellulose is a crystalline structure composed of β-D-glucopyranose monomers [5,6]. It is a polymer chain with a degree of polymerization (DP) around 10000 [3,5]. The different DPs of celluloses influence their properties. A larger DP relates to superior mechanical and thermal properties [8].

The development of nanotechnology in last two decades has increased the interest in the properties of nanocellulose materials. Nanocellulose, which has a diameter in the range 1-100 nm, has high transparency, low density, high contact surface area, good mechanical properties, and is environmentally friendly [4,8].

Nanocellulose fibers from a number of sources including kenaf [6], oil palm empty fruit bunch fiber (OPEFB) [9-11], pineapple leaf fiber (PLF) [12], mengkuang leaves [13], waste sugarcane bagasse [14], wheat straw [15], and bacterial cellulose [39] have been isolated in recent times. In each case, isolation of nanocellulose fiber was achieved by chemical removal of lignin and hemicellulose. This treatment is used to obtain highly purified cellulose [6]. Generally, nanocellulose thus isolated is in the form of a transparent colloid suspension [8,16,17].

To obtain nano size fiber, many researchers use mechanical treatments such as high-pressure homogenization (HPH) [6,7,18], sonication [10,19,39], ball mill [20], high-speed blender [21,22], and ultrafine grinder [23,24]. However, mechanical treatment alone is not sufficient to separate lignin, hemicellulose, and cellulose. Chemical treatment and sonication combined can produce pure nanocellulose. Sonication treatment has been found to be the simplest method to obtain pure nano-size cellulose fiber in suspension after chemical treatments [10,19].

Water hyacinth, a common aquatic plant, commonly contains 60 % cellulose fiber [27]. However, the cellulose fiber content may depend on the growing environment. In Indonesia, this plant grows quickly producing 125 tons/ha in 6 months [25,26]. WHF nanocellulose was first isolated using a cryo-crushing method to obtain cellulose nanofiber with diameter around 25 nm and length in the range of micrometers [28]. High shear homogenization method has also been used resulting in an aggregate particle form with a diameter of 25-40 nm; the duration of high shear homogenization damaging cellulose chain structure [1].

While many studies have investigated the properties of nanocellulose from other sources as far as the authors are

*Corresponding author: abral@ft.unand.ac.id

aware, information regarding the characterization of WHF nanofibers is limited to a single study using SEM, TGA, and FTIR [28]. Hence this study explores a wider range of properties of highly purified samples of WHF after each stage of production in more depth. TEM and particle size analysis were used to observe the morphology of WHF and determine the distribution diameter size after sonication. Chemical composition, XRD, and moisture absorption were also measured.

Experimental

Materials

WH plants were obtained from a local river in Payakumbuh, Indonesia. The WH stem was separated from root and leaves before being processed into cellulose fiber [1]. Distilled water, sodium hydroxide, sodium chloride, acetic acid, and hydrochloric acid were used in WHF isolation. All chemical reagents were analytical grade and obtained from Agriculture Technology Laboratory, Andalas University, Indonesia.

Preparation of WHF

The WH stem was prepared as reported by previous reports [1,10]. It was dried under the sun for 3 days and cut about 1 cm long before chemical treatment.

Pulping in Digester

The WH stem and 15 % sodium hydroxide solution were mixed in the ratio 1:10. The WH stem was cooked in a high-pressure digester for 6 h at 4 bars pressure and 130 ^{o}C. The resulting WHF was rinsed with distilled water until pH 7 and dried under the sun for 2 days until it became paper-like. A 10 g WHF paper (dry basis) was mixed with 5 % sodium hydroxide at 60 ^{o}C for 4 h. This pulping method is more environmentally friendly than sulfate pulping.

Bleaching Process

The bleaching process was done by soaking the fibers in a 4:1 mixture of sodium chlorite and acetic acid at 60 ^{o}C for 2 h. During this process, the color of WHF changed from brown to white. The bleaching fiber was neutralized with distilled water until pH 7. This treatment was done to remove the residual lignin completely.

Acid Hydrolysis

To obtain a smaller and uniform size of cellulose fibers, acid hydrolysis was done by two steps. The aim of this process was to increase the crystallinity of the WHF cellulose. The bleaching of WHF was conducted using 5M hydrochloric acid at 60 ^{o}C and 500 rpm for 20 h. Then the fiber was hydrolyzed again with 3.5M hydrochloric acid at 60 ^{o}C and 500 rpm for another 20 h. The hydrolyzed fiber was rinsed with distilled water until pH 7 (neutral). This double hydrolysis is gentler on the fiber and made the WHF easier to process with sonication compared to a single sulfuric acid hydrolysis process.

Sonication

This was conducted with 0.5 % cellulose WHF (from acid hydrolysis process) dispersed in 100 m*l* of distilled water. An ultrasonic cell crusher SJIA-1200W was used to sonicate this suspension at 20 kHz and 600 W for 1 h until the nanocellulose fiber was completely dissolved. The temperature of WHF cellulose suspension was kept under 50 ^{o}C. The resulting nanocellulose WHF suspension is shown in Figure 2(d).

Characterization

Chemical Composition

The American Standard Testing Materials (ASTM) 1104-56, Technical Association of the Pulp and Paper Industry (TAPPI) T9M-54 and TAPPI T13M-54 standards were used to measure the holocellulose (cellulose and hemicellulose), cellulose, and lignin content in the fiber. Raw WHF, pulping-digester, and acid hydrolysis fiber samples were tested. Each sample was 3 g of dried material prepared for testing according to the standard.

Scanning Electron Microscopy (SEM)

SEM was used to observe the morphological surface WHF; raw, pulped, bleached, and after acid hydrolysis. An SEM Hitachi 3400 N instrument was used in this study. The operation voltage was 10 kV.

Particle Size Analysis (PSA)

Diameter size distribution of the nanocellulose WHF suspension was conducted using a Beckman Coulter Delsa Nano C. The test was carried out at room temperature (25 ^{o}C), viscosity 0.88 cP, scattering intensity (SI): 9581 cps, refractive index (RI): 1.3332. The data was processed by using Delsa Nano Software.

Transmission Electron Microscopy (TEM)

TEM characterization to measure the diameter size distribution and morphological of nanocellulose WHF used TEM JEM-JEOL 1400 at 100 keV. A 5 m*l* nanocellulose WHF suspension (0.5 % WHF content) drip was cast onto a carbon coated grid. The dried nanocellulose suspension was observed at room temperature.

X-ray Diffraction (XRD)

Raw WHF and all treated samples were formed into paper sheets. They were dried completely in the oven at temperature 60 ^{o}C for 3 h before XRD measurement. The dried fiber sheets were cut to size 0.5×0.5 cm. XRD characterization was carried out by using a PAN analytical Xpert PRO instrument using 40 kV and 35 mA. Diffraction intensity was recorded from (2θ=10-80 ^{o}) with λ=0.154 nm. The crystallinity index calculation was measured using peak height as shown by equation (1) [29]:

$$I_{cr} = \frac{I_{200} - I_{am}}{I_{200}} \quad (1)$$

where I_{200} is maximum diffraction peak intensity at 2θ=22.6 ^{o} (the crystalline area). I_{am} is the diffraction peak at 2θ=18 ^{o} (the amorphous area). The crystal thickness, D, was measured with Derby Scherer's equation (2) [16]:

$$D = \frac{k\lambda}{\beta \cos\theta} \quad (2)$$

where k is form factor (0.89) and β is FWHM (Full Width Half Maximum) of maximum intensity (I_{200}) in radians.

Fourier Transform Infrared (FTIR)

FTIR using Perkin-Elmer Frontier was used to determine the functional groups of raw WHF then after pulping, bleaching, acid hydrolysis, and sonication. FTIR spectrum was recorded from wavenumber 600-4000 cm^{-1} using 1 cm × 1 cm samples mixed with KBr powder and pressed to become the transparent KBr-sample pellet.

Thermogravimetric Analysis (TGA)

Thermal characteristics of WHF from each treatment step were tested by using a Mettler Toledo TGA/DSC1 instrument. Thermal characterization was carried out from 30-600 ^{o}C. The heating rate was 10 ^{o}C/min in nitrogen at atmospheric pressure. The weight of sample for testing was 7-10 mg.

Moisture Absorption

Before testing, 1×1 cm untreated (WHF) and treated fiber paper squares were dried in the drying oven at 60 ^{o}C for 2 days, and then the dried samples were placed in a moisture chamber with 75 % relative humidity (RH) and 25 ^{o}C. Five repeats for each treatment were used. The sample was weighted every 30 min by using analytical balance (Kenko brand precision 0.001 g). The moisture absorption value was calculated by the equation (3):

$$Moisture\ absorption = \frac{W_t - W_0}{W_0} \times 100\% \quad (3)$$

where W_t is the final weight and W_0 the initial weight of the sample.

Results and Discussion

Chemical Compositions of WHF

The chemical composition of the WHF after each stage of processing is given in Table 1. The raw WHF contains 43.01 % cellulose, 29.13 % hemicelluloses, and 6.9 % lignin. The high lignin content is due to the close bonding of lignin and hemicellulose fibers. The cellulose content is similar to that of wheat straw (43.2 %) [15], arecanut husk (34.2 %) [16], coir fiber (39.3 %) [30], bamboo (41.8 %), and wood (46.4 %) [19].

Table 1. Chemical composition of fiber in each stage treatment

Sample	Hemicellulose (%)	Cellulose (%)	Lignin (%)	Ash (%)
Raw WHF	29.13	43.01	6.9	3.8
Pulping-digester	9.40	61.09	3.04	-
Acid hydrolysis	5.80	77.35	2.56	-

After pulping-digestion treatment, the content of lignin and hemicellulose decreased due to the broken ether linkages between lignin and hemicellulose in the WHF [2,13,14,16]. This confirms that the pulping-digestion process efficiently removed the lignin and hemicellulose as has been demonstrated in a previous study [16]. This data was also supported by SEM observation and FTIR characterization.

Pulping-digesting followed by acid hydrolysis almost doubled the cellulose content of the fiber from the raw state. This is due to the destruction of hydrogen bonds between cellulose and hemicellulose complex chains and decomposition of hemicellulose [12,13,30]. This phenomenon increased the crystallinity index [6]. This result is in agreement with XRD characterization and with previous studies [16,30].

Morphological Surface Analysis

Figure 1 shows morphological analysis of untreated and treated WHF. The untreated (raw WHF) is shown in Figure 1(a). The main structure of raw WHF is composed of microfibrils which are tightly linked by a mass of adhesive substances, possibly waxes, and oils, which also give the WHF a smooth appearance [2,14,16].

After pulping-digestion, this mass has been broken up releasing individual microfibril with diameter around 10-40 μm as shown in Figure 1(b). This is due to the hydrolyzed hemicellulose and its solubility in water. Some of the lignin was depolymerized and removed [2].

Figure 1(c) shows the morphology of the bleached fiber. The surface looks pale showing that the non-cellulosic content such as lignin, hemicellulose, wax, and oil has been removed. This non-cellulosic content was rapidly oxidized and degraded by chlorine gas [12,16].

After bleaching, the fiber was treated by acid hydrolysis. This results in a reduction in fiber size. The fiber appears to be individual microfibrils about 2 μm wide and 6 μm long (Figure 1(d)). This result, that has been observed by previous studies, is due to depolymerization [2,30,31] and also supported by chemical composition analysis which indicates that cellulose content increased after hydrolysis (see Table 1).

Distribution Size after Sonication

After acid hydrolysis, the fiber was sonicated to reduce fiber diameter size [19]. Figure 2(a) shows TEM images of WHF nanocellulose after 1 h sonication. Diameter and length distribution of WHF nanocellulose are presented in Figure 2(b) and 2(c), respectively. The average diameter and length of nanocellulose WHF were 15.16 and 147.4 nm, respectively. The final product of WHF nanocellulose was a suspension (Figure 2(d)). Particle size analysis shows the

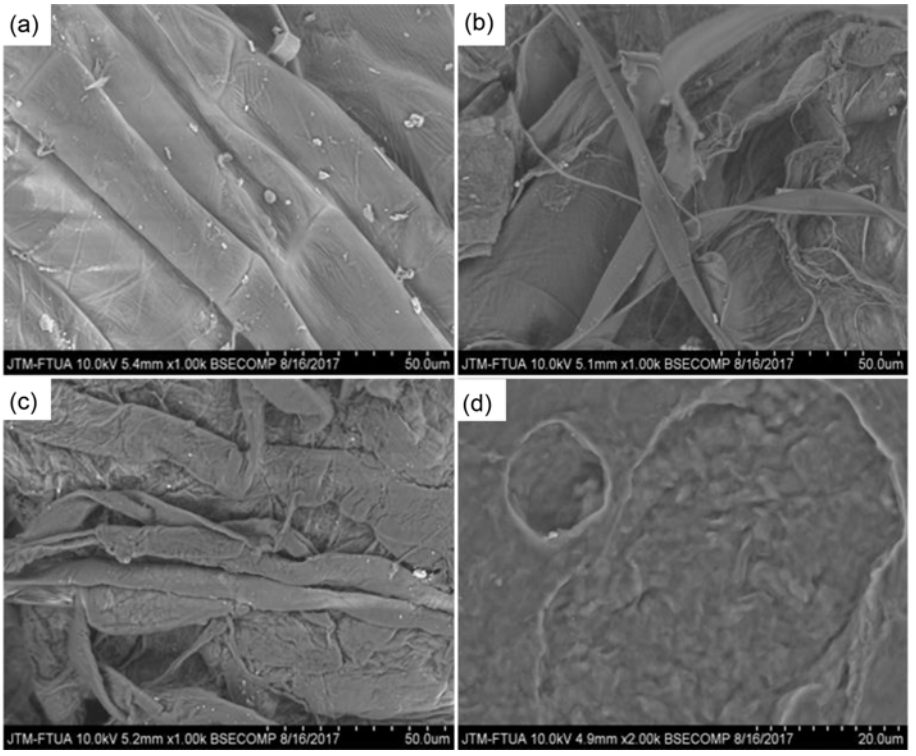

Figure 1. Surface morphology of fiber at diffrent treatment stages; (a) untreted (raw WHF), (b) pulping-digester, (c) bleaching, and (d) acid hydrolysis.

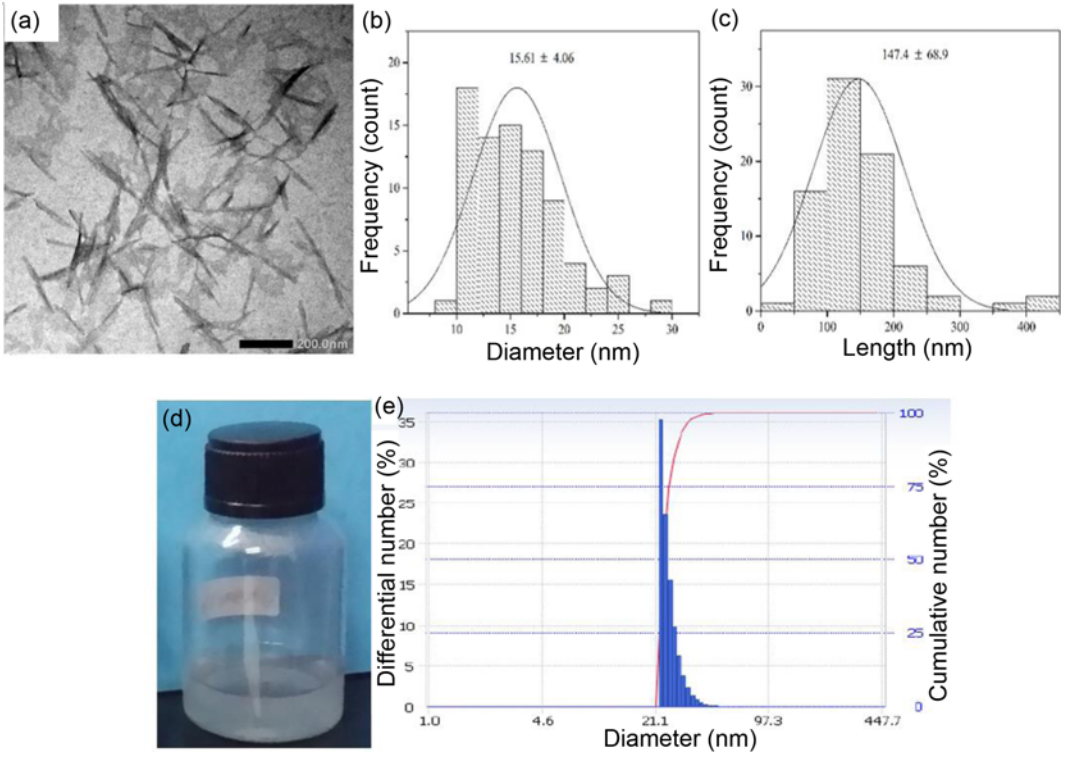

Figure 2. (a) TEM image of WHF after sonication 1 h, (b) diameter, (c) length distribution, final product of nanocellulose WHF, and (e) PSA analysis.

diameter of WHF nanocellulose was around 25 nm (Figure 2(e)). This result was in agreement with TEM characterization and similar to previous reports [13,14].

Acid hydrolysis separates the cellulose fibers by destroying the hydrogen bonds between the cellulose polymers hence reducing the diameter of the fibers. The forces produced during sonication are sufficient to break some of the bonds between the glucose unit resulting in depolymerization and shorter fiber lengths in the nanometer range.

Crystallinity Index

XRD characterization was used to determine the crystallinity index, crystal thickness, and the distance between the lattices as in Table 2. Figure 3 shows the XRD characteristics of the untreated (raw WHF) and treated fiber. There are two characteristic peaks in the range of 2θ=(15-30 ^{o}). The first peak at 2θ=18 ^{o} corresponds to the amorphous region, whereas the second peak at 2θ=22 ^{o} indicates the presence of the crystalline region. This characteristic is identical to that of cellulose type I. This phenomenon was caused by the interaction between the hydroxyl group bonds in the cellulose forming a crystalline structure [1,16]. In Table 2, the untreated fiber (raw WHF) showed a crystallinity index of about 5 %. This value was the lower than that of treated fiber indicating that amorphous components such as lignin and hemicellulose were still present in raw WHF [2,15,16]. This result was also supported by FTIR characterization, chemical composition, and SEM.

Table 2. Crystallinity index, crystal thickness, and *d*-spacing at various treatments

Sample	Crystallinity index (%)	Crystal thickness (nm)	*d*-spacing (Å)
Raw WH fiber	5.00	0.043	4.030
Pulping-digester	58.55	0.221	3.934
Bleaching	73.15	0.209	3.862
Acid hydrolysis	84.87	0.248	3.870
Sonication 1 h	80.45	0.228	3.883

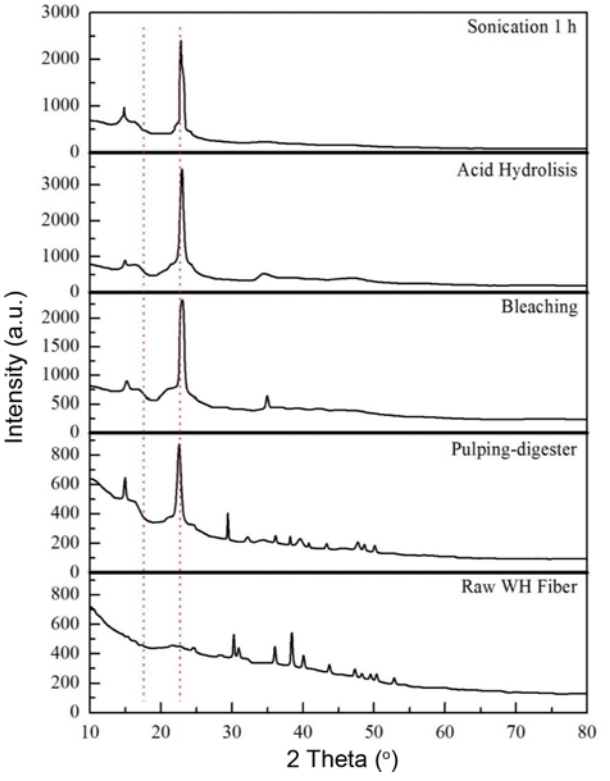

Figure 3. XRD of samples tested with diffrent treatments.

The treated fiber, however, had one sharp peak at 2θ=22 ^{o}. The highest peak was measured in the acid hydrolysis treated fiber. The value of this crystallinity index was 88 % due to the degradation of cellulose by acid penetration into the amorphous region of the cellulose fiber [2,12,13,16].

After 1 h sonication, the crystalline index decreased due to the destruction of the cellulose chains [19]. This phenomenon was supported by TEM observations that show the nanocellulose comprises of individual short nanofibrils.

The crystal thickness increased with increasing crystallinity index (see Table 2). The crystal thickness increased sharply after acid hydrolysis and sonication which results in an increase in the contact surface area of the crystalline structure. Similar results were also reported by other researchers [1,16]. The distance between the lattices of atoms was also reduced after the chemical and mechanical treatment [15,16]. This result was supported by the crystalline domain area value.

Functional Group Analysis

Natural fiber comprises of amorphous lignin, hemicellulose, and crystalline cellulose. These components can be characterized by looking at the functional groups [31]. Figure 4 shows the infrared spectra of WHF at each stage of processing. There are four main peaks in each sample in the wavenumber area 3500-3000 cm^{-1}, 3000-2800 cm^{-1}, 1750-1200 cm^{-1}, and 1100-1000 cm^{-1}.

The characteristic peak in the range 3500-3000 cm^{-1} corresponds to the stretching of -OH due to hydrogen bond interaction with hydroxyl groups [1,2,40]. The spectra associated with C-H stretching appeared in all samples at wavenumber 3000-2800 cm^{-1}. This cluster indicates that all samples have aliphatic saturated components [9].

The characteristic peak of -OH bending in the adsorbed water appears in all samples around 1630 cm^{-1}. Untreated fiber had lower transmittance than the treated fibers. This result was supported by moisture absorption testing which indicated that nanocellulose WHF after sonication has a low moisture absorption percentage.

The untreated fiber also exhibited a peak at the 1721 cm^{-1} due to the presence of C=O bonds indicating the presence of lignin and hemicellulose [2,30]. After chemical and mechanical

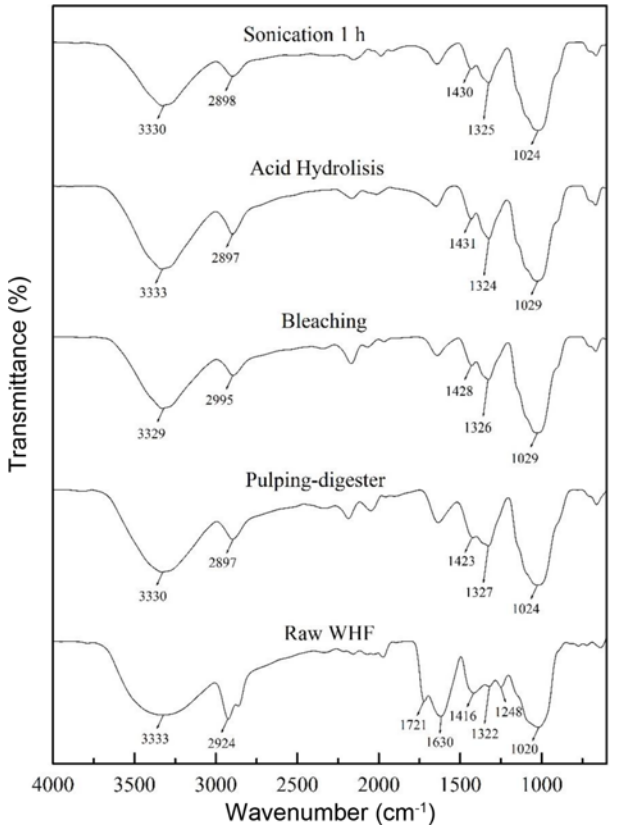

Figure 4. FTIR of samples tested with diffrent treatments.

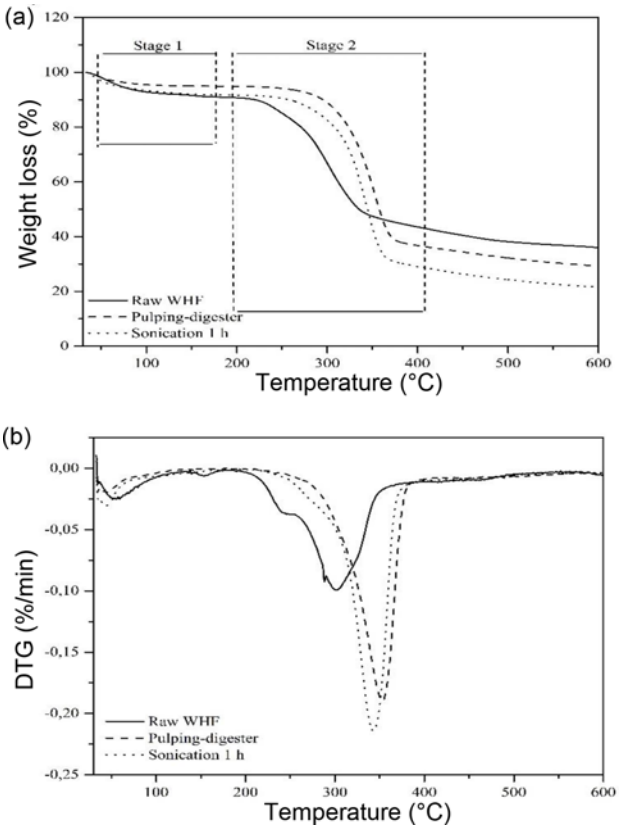

Figure 5. (a) TGA and (b) DTG of raw WHF, pulping-digester, and sonication 1 h, respectively.

treatment, this peak did not appear.

The aromatic ring vibration of lignin occurs in the range 1500-1200 cm^{-1} [2,16,31]. This characteristic peak appeared at 1248 cm^{-1} in untreated fiber but not in the treated fiber indicating that the chemical treatment successfully removed the lignin component increasing the cellulose component. This result was also supported by chemical composition analysis.

In the wavenumber range of 1020-1030 cm^{-1} there is the characteristic peak due to the stretching of C-O-C of the pyranose ring in cellulose [16,31]. This peak appeared in all samples.

Thermal Stability

Thermogravimetric analysis was used to study the thermal stability of WHF after each step of treatment. Figure 5(a) shows the TGA curves of the samples. There are two main degradation stages as reported by previous researchers [31-33].

Stage 1 (initial weight loss) occurs in the temperature range of 46-173 ^{o}C. At this stage, weight loss of fiber was 3-8 % due to the evaporation of water and other volatile components [32,34,36]. The corresponding part of the DTG curve shows a small trough around 100 ^{o}C for the same reason. The DTG curve (Figure 5(b)) for raw WHF has a sharper trough than the curve for treated fiber. Weight loss at this stage was 8 % due to the less compact more swollen structure [15,26,32]. Fiber treated with pulping-digestion and sonication lost less weight as the lignin and hemicellulose had been removed as reported in previous research [31,34].

Stage 2 (active pyrolysis) occurs at 191-406 ^{o}C. A large weight loss occurred during this stage. Hemicellulose and lignin degrade at these temperatures [32,33]. This stage was divided into two regions; (191-300 ^{o}C) and (300-406 ^{o}C).

Raw WHF, with a degradation temperature of 225 ^{o}C, loses more of its weight at the beginning pyrolysis process (191-300 ^{o}C) than the treated fiber with degradation temperatures of 280 and 250 ^{o}C for pulped-digested fiber and sonicated fiber, respectively. The hemicellulose and lignin content in raw WHF results in this lower thermal stability as they have lower thermal resistance than cellulose [33,34].

Contrastingly, in the second region (300-406 ^{o}C) raw WHF loses less weight than treated fiber due to the slow degradation rate of hemicellulose and lignin as these compounds have mostly been degraded at lower temperatures [15,32,34,35].

The corresponding TGA result for stage 2 shows a dominant peak at 250-400 ^{o}C indicating the pyrolysis process

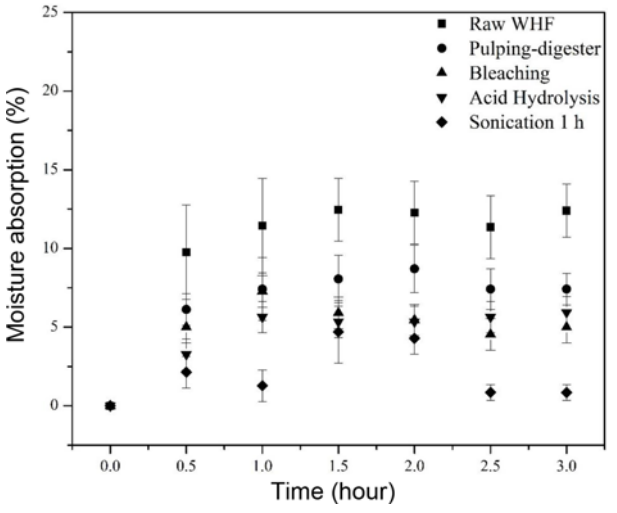

Figure 6. Moisture absorption of all samples tested.

of the WHF. During this process, lignin and hemicellulose were lost and the cellulose chain of WHF was broken. Some of the fiber is broken down and lost as CO_2 and volatile hydrocarbons [33]. However, the thermal stability of the treated fiber was better than the untreated fiber.

Figure 5(a) (from stage 1-2) indicates that the sonicated nanocellulose WHF has lower thermal stability than the pulped-digested microcellulose as the cellulose chains in the nanocellulose are shorter. This conclusion is supported by TEM and XRD observation.

Moisture Absorption

Figure 6 displays the moisture absorption of WHF at various stages of treatment at RH 75 % and 25 ^{o}C over 3 h. It is evident that moisture saturation was reached in all samples after about 2 h.

After 3 h the moisture absorption of raw, pulped-digested, bleached, acid hydrolysis treated, and sonicated fiber was 12.85, 7.41, 5.00, 5.93, and 0.85 %, respectively. Raw WHF shows the highest moisture absorption indicating higher porosity than treated fiber. The low result for the treated samples was unexpected and is probably due to the sample preparation methods. Sonicated fiber has the lowest moisture absorption value due to the difficulty of water molecules interacting with the cellulose chain. Sonication breaks the cellulose chain down into more compact cellulosic molecules with less nano-size porosity [37,38]. This result is supported by FTIR results in the wavenumber range of 1630 cm^{-1}.

Conclusion

High purity nanometer-sized cellulose was successfully obtained from WHF after a series of mechanical and chemical treatments. SEM and TEM document the morphological change of the WHF before and after treatment. The WHF disintegrated during bleaching and depolymerized during acid hydrolysis. TEM and particle size analysis show that nano-sized fibers were produced by sonication. Acid hydrolysis was effective in reducing the lignin, hemicellulose content. A very high value for crystallinity index (84.87 %) was achieved at this stage but crystallinity index decreased on sonication. The low moisture absorption and high crystallinity index values obtained suggest that sonicated WHF so treated could be an effective reinforcing material for biocomposite film and hence be used along with a suitable starch in the manufacture of environmentally friendly packaging.

Acknowledgement

This research was funded by Directorate General of Higher Education Ministry of National Education (KEMENRISTEK DIKTI), Indonesia, with project name The Research of Master Program Leading to Doctoral Degree for Excellent Students (PMDSU Batch-2) in the year of 2017. We also thank Mrs. Fay Farley for her proofreading.

References

1. M. Asrofi, H. Abral, A. Kasim, and A. Pratoto, *J. Metastable Nanocrystalline Mater.*, **29**, 9 (2017).
2. E. Abraham, B. Deepa, L. A. Pothan, M. Jacob, S. Thomas, U. Cvelbar, and R. Anandjiwala, *Carbohydr. Polym.*, **86**, 1468 (2011).
3. M. J. John and S. Thomas, *Carbohydr. Polym.*, **71**, 343 (2008).
4. K. G. Kavelin, Master Thesis, Budapest University of Technology and Economics, Russia, 2015.
5. H. P. S. Abdul Khalil, Y. Davoudpour, Md. N. Islam, A. Mustapha, K. Sudesh, Rudi Dungani, and M. Jawaid, *Carbohydr. Polym.*, **99**, 649 (2014).
6. M. Jonoobi, J. Harun, A. Shakeri, M. Misra, and K. Oksman, *BioResources*, **4**, 626 (2009).
7. Y. Wang, X. Wei, J. Li, F. Wang, Q. Wang, J. Chen, and L. Kong, *Fiber. Polym.*, **16**, 572 (2015).
8. D. Klemm, F. Kramer, S. Moritz, T. Lindstrom, M. Ankerfors, D. Gray, and A. Dorris, *Angew. Chem. Int. Ed.*, **50**, 5438 (2011).
9. N. S. Lani, N. Ngadi, A. Johari, and M. Jusoh, *J. Nanomater.*, **2014**, 1 (2014).
10. F. Fahma, S. Iwamoto, N. Hori, T. Iwata, and A. Takemura, *Cellulose*, **17**, 977 (2010).
11. M. K. M. Haafiz, A. Hassan, Z. Zakaria, and I. M. Inuwa, *Carbohydr. Polym.*, **103**, 119 (2014).
12. B. M. Cherian, A. L. Leao, S. F. de Souza, S. Thomas, L. A. Pothan, and M. Kottaisamy, *Carbohydr. Polym.*, **81**, 720 (2010).
13. R. M. Sheltami, I. Abdullah, I. Ahmad, A. Dufresne, and H. Kargarzadeh, *Carbohydr. Polym.*, **88**, 772 (2012).
14. A. Mandal and D. Chakrabarty, *Carbohydr. Polym.*, **86**,

1291 (2011).
15. Alemdar and M. Sain, *Bioresour. Technol.*, **99**, 1664 (2008).
16. S. J. Chandra, N. George, and S. K. Narayanankutty, *Carbohydr. Polym.*, **142**, 158 (2016).
17. Salas, T. Nypelo, C. Rodriguez-Abreu, C. Carrillo, and O. J. Rojas, *Curr. Opin. Colloid Interface Sci.*, **19**, 383 (2014).
18. J. Li, X. Wei, Q. Wang, J. Chen, G. Chang, L. Kong, J. Su, and Y. Liu, *Carbohydr. Polym.*, **90**, 1609 (2012).
19. W. Chen, H. Yu, Y. Liu, P. Chen, M. Zhang, and Y. Hai, *Carbohydr. Polym.*, **83**, 1804 (2011).
20. Solikhin, Y. S. Hadi, M. Y. Massijaya, and S. Nikmatin, *Waste Biomass Valorization*, **8**, 2451 (2017).
21. K. Uetani and H. Yano, *Biomacromolecules*, **12**, 348 (2011).
22. M. Asrofi, H. Abral, A. Kasim, and A. Pratoto, *IOP Conf. Ser. Mater. Sci. Eng.*, **204**, 012018 (2017).
23. T. Taniguchi and K. Okamura, *Polym. Int.*, **47**, 291 (1998).
24. O. Nechyporchuk, F. Pignon, and M. N. Belgacem, *J. Mater. Sci.*, **50**, 531 (2014).
25. T. Istirokhatun, N. Rokhati, R. Rachmawaty, M. Meriyani, S. Priyanto, and H. Susanto, *Procedia Environ. Sci.*, **23**, 274 (2015).
26. H. Abral, D. Kadriadi A. Rodianus, P. Mastariyanto, Ilhamdi, S. Arief, S. M. Sapuan, and M. R. Ishak, *Mater. Des.*, **58**, 125 (2014).
27. A. F. Abdel-Fattah and M. A. Abdel-Naby, *Carbohydr. Polym.*, **87**, 2109 (2012).
28. M. T. Sundari and A. Ramesh, *Carbohydr. Polym.*, **87**, 1701 (2012).
29. S. Park, J. O. Baker, M. E. Himmel, P. A. Parilla, and D. K. Johnson, *Biotechnol. Biofuels*, **3**, 1 (2010).
30. Abraham, B. Deepa, L. A. Pothen, J. Cintil, S. Thomas, M. J. John, R. Anandjiwala, and S. S. Narine, *Carbohydr. Polym.*, **92**, 1477 (2013).
31. J. I. Moran, V. A. Alvarez, V. P. Cyras, and A. Vazquez, *Cellulose*, **15**, 149 (2008).
32. H. Yang, R. Yan, H. Chen, D. H. Lee, and C. Zheng, *Fuel*, **86**, 1781 (2007).
33. A. R. Martin, M. A. Martins, O. R. R. F. Da Silva, and L. H. C. Mattoso, *Thermochim. Acta*, **506**, 14 (2010).
34. X. Chen, J. Yu, Z. Zhang, and C. Lu, *Carbohydr. Polym.*, **85**, 245 (2011).
35. Awal, S. B. Ghosh, and M. Sain, *J. Therm. Anal. Calorim.*, **99**, 695 (2010).
36. S. Y. Lee, D. J. Mohan, I. A. Kang, G. H. Doh, S. Lee, and S. O. Han, *Fiber. Polym.*, **10**, 77 (2009).
37. H. Abral, G. J. Putra, M. Asrofi, J. W. Park, and H. J. Kim, *Ultrason. Sonochem.*, **40**, 697 (2018).
38. M. Asrofi, H. Abral, Y. K. Putra, S. M. Sapuan, and H. J. Kim, *Int. J. Biol. Macromol.*, **108**, 167 (2018).
39. H. Abral, V. Lawrensius, D. Handayani, and E. Sugiarti, *Carbohydr. Polym.*, **191**, 161 (2018).
40. H. Abral, M. H. Dalimunthe, J. Hartono, R. P. Efendi, M. Asrofi, E. Sugiarti, S. M. Sapuan, J. W. Park, and H. J. Kim, *Starch/Staerke*, https://doi.org/10.1002/star.201700287 (2018).